

Dalton Transactions

Accepted Manuscript



This is an *Accepted Manuscript*, which has been through the Royal Society of Chemistry peer review process and has been accepted for publication.

Accepted Manuscripts are published online shortly after acceptance, before technical editing, formatting and proof reading. Using this free service, authors can make their results available to the community, in citable form, before we publish the edited article. We will replace this *Accepted Manuscript* with the edited and formatted *Advance Article* as soon as it is available.

You can find more information about *Accepted Manuscripts* in the [Information for Authors](#).

Please note that technical editing may introduce minor changes to the text and/or graphics, which may alter content. The journal's standard [Terms & Conditions](#) and the [Ethical guidelines](#) still apply. In no event shall the Royal Society of Chemistry be held responsible for any errors or omissions in this *Accepted Manuscript* or any consequences arising from the use of any information it contains.

A Hydrothermal Stable Zn(II)-based Metal-Organic Framework: Structural Modulation and Gas Adsorption

Xiuling Zhang,^a Yong-Zheng Zhang,^a Da-Shuai Zhang,^{a*} Baoyong Zhu,^a
Jian-Rong Li^{b*}

By the solvothermal reaction of a triangular ligand, 2,4,6-tris-(4-carboxyphenoxy)-1,3,5-triazine (H₃tcpt) with Zn(NO₃)₂ in N,N'-dimethylacetamide/acetonitrile/H₂O (v/v/v = 1:1:1) mixed solvent, a two-fold interpenetrated three-dimensional (3D) porous metal-organic framework, [Zn₂(tcpt)OH]·solvents (**1**-solvents), with a rare paddlewheel second building unit (SBU) Zn₂(COO)₃, was synthesized and characterized. It was found that the single 3D structure of **1** forms when two-dimensional layers, which are constructed by tcpt³⁻ bonding the paddlewheel SBUs, are linked by -OH group alone the axial sites of the SBUs. Compared with reported Zn(II)-based partners with this ligand, synthesis conditions, particularly used solvents clearly played a key role in the formation of different SBUs, thereby resulting distinct MOFs with the same ligand. Particularly, **1** features good water and thermal stability, and can withstand acid aqueous solution of pH values ranging from 5 to 12. In addition, **1** performs good adsorption ability towards H₂ (2.21 wt% at 77 K and 1 atm), and can selectively adsorb CO₂ from CH₄ and N₂, in spite of its relative low void volume (36.8%), suggesting potential application in gas storage and separation.

1. Introduction

As an emerging porous materials, metal-organic frameworks (MOFs) have been widely researched these years. Due to their interesting and various structures and excellent chemical/physical properties, MOFs could be utilized in a lot of areas, such as gas storage, separation, catalysis, magnetism, and luminescence.¹ However, to apply MOFs in practices, there are still many issues to be resolved, among them the stability of framework, especially under high temperature and water environment are particularly significant. With this purpose, some methods have been developed to enhance the stability of MOFs, such as surface carbonization,² fluorine modified pores,³ and the construction of multi-interpenetrated frameworks.⁴ Since MOFs are composed of organic linkers and secondary building unit (SBU), the regulation of the two parts is vital to form stable structures. Considering that the selection of organic linkers is relatively controllable, modulating the *in-situ* formed SBUs is thus a

^b Beijing Key Laboratory for Green Catalysis and Separation and Department of Chemistry and Chemical Engineering, Beijing University of Technology, Beijing 100124, P. R. China. E-mail: jrli@bjut.edu.cn

conceivable way for stability enhancing. On the other hand, the formation of a SBU depends on various factors,⁵⁻⁷ e.g. reaction temperature, solvents, and pH. Under different conditions, MOFs with different structures and properties are usually obtained.

In our effort to design and synthesize new MOFs through controlling reaction conditions, a tritopic ligand, 2,4,6-tris-(4-carboxyphenoxy)-1,3,5-triazine (H₃tcpt) reported by several other groups for synthesizing MOFs was used.^{6,7} From the literatures, it was found that this ligand could generate a two-dimensional (2D) layer structural MOF, [Zn₃(L)₂(H₂O)₂]·3H₂O·TEA·2DMF⁶ with Zn₃(COO)₆ SBUs in mixed DMF/EtOH/H₂O solvent. While, the 2D layers could be linked by *in-situ* produced formate species to form a three-dimensional (3D) framework (SNU-100)⁷ when the used solvent was changed to pure DMF. Clearly, solvents play a key role in the formation of these MOFs.

In this work, we used different solvent of DMA/acetonitrile/ H₂O (v/v/v = 1:1:1), a new 3D MOF, [Zn₂(tcpt)OH]·solvents (**1**-solvents) was synthesized, in which an unusual paddlewheel SBUs Zn₂(COO)₃ was found. Unlike common paddlewheel SBUs⁶⁻⁸ consisting of four carboxyl groups, this SBU is just three. Different from above

^a Key Laboratory of Coordination Chemistry, Functional Materials in Universities of Shandong (Dezhou University), Dezhou, 253023 P. R. China. E-mail: dashuai_74@163.com

mentioned two MOFs with this ligand, in **1** the 2D layers assembled by H₃tcpt ligands and Zn₂(COO)₃ SBUs are further linked by –OH groups to finally form a 3D interpenetrated framework with excellent stability. Moreover, **1** performs good adsorption ability towards H₂ (2.21 wt% at 77 K and 1 atm), and can selectively adsorb CO₂ from CH₄ and N₂, in spite of its relative low void volume (37.7%), suggesting potential application in gas storage and separation.

2. Experimental section

2.1 Materials and measurements

The ligand 2,4,6-tris(4-carboxyphenoxy)-1,3,5-triazine (H₃tcpt) was synthesized according to the literature method.⁹ All commercially available chemicals and solvents are of reagent grade and were used as received without further purification. The IR spectra were recorded on a Thermo Nicolet IR200 FT-IR spectrometer as KBr pellets (4000–400 cm⁻¹). Thermogravimetric analyses (TGA) were carried out on a SHIMADZU DTG-60 thermoanalyzer under nitrogen with a heating rate of 5 °C min⁻¹ from room temperature to 700 °C. Powder X-ray diffraction (PXRD) measurements were performed on a SHIMADZU XRD-6000 X-ray diffractometer using Cu-K α radiation ($\lambda = 0.1542$ nm), in which the X-ray tube was operated at 40 kV and 40 mA at room temperature. The temperature-dependent X-ray powder diffraction patterns were recorded in a Bruker D8 diffractometer at 40 kV and 40 mA with a Cu-target tube and a graphite monochromator. The elemental analysis for C, H and N were performed on an Elementar Vario Micro Cube analyzer. N₂, H₂, CO₂ and CH₄ adsorption measurements (up to 1 bar) were performed on an Autosorb-3.0 (Quantachrome) volumetric analyzer. All these gases are extra pure quality (99.999% purity).

2.2 Synthesis of **1**-solvents

Zn(NO₃)₂·6H₂O (0.2 mmol, 59.4 mg) and H₃tcpt (0.1 mmol, 48.9 mg) were added to a mixed solvent of N,N'-dimethylacetamide (DMA)/ acetonitrile (ACN)/H₂O (v/v/v = 1:1:1, 6 mL) with two drops of tetrafluoroboric acid (HBF₄, 48%) in a sealed glass vial. Then the obtained mixture was ultrasonicated to dissolve and then heated at 90 °C for 48 h. After cooling to room temperature, prism colorless crystals were collected by filtration, and washed with H₂O and DMA (Yield: 43.5% based on H₃tcpt). Anal. calcd (%) for the activated sample (see below) C₂₄H₁₃N₃O₁₀Zn₂ (%): C, 45.46; H, 2.07; N, 6.63. Found: C, 45.51; H, 2.01; N, 6.57.

2.3 X-ray crystallography

Diffraction intensity data of the single crystal of complex was collected on a Agilent Technologies SuperNova diffractometer at 100 K equipped with a mirror monochromated Cu-K α radiation ($\lambda = 1.54184$ Å) by using a ω -scan mode. Empirical absorption correction using spherical harmonics, implemented in SCALE3 ABSPACK scaling algorithm.¹⁰ All the structures were solved by direct methods and refined by full-matrix least-squares methods on F² using the program SHELXL-2014.¹¹ The single suite WINGX¹² and Olex2 1.2-alpha¹³ were used as integrated systems for the crystallographic programs. All non-hydrogen atoms were refined anisotropically. The hydrogen atoms were located by geometrically calculations, and their positions and thermal parameters were fixed during the

structure refinement. For this compound, the volume fractions of disordered solvent in the pores could not be modeled in terms of atomic sites and were treated using the MASK routine in the Olex2 software package. The coordination O atoms of hydroxy in **1**-solvents were disordered, and treated by occupancies refinement of the disordered atoms. Crystallographic data and refinement parameters are listed in Table S1, and selected bond lengths and angles are listed in Table S2. CCDC-1414115 contains the supplementary crystallographic data of **1**. These data can be obtained free of charge from the Cambridge Crystallographic Data Centre via www.ccdc.cam.ac.uk/data_request/cif.

2.4 Water stability test

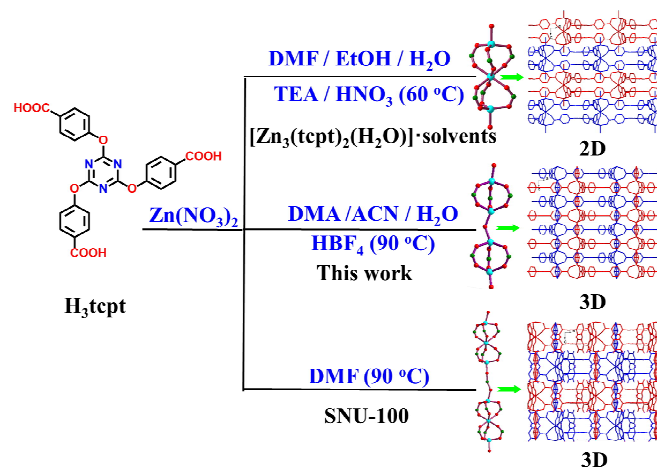
Seven as-synthesized bulk samples in the same batch (45 mg) were soaked in pH = 5, 6, 7, 8, 9, 11, and 12 aqueous solutions for 48 h, respectively. After that, the samples were collected by decanting and dried in air, then the structural integration were checked.

2.5 Gas adsorption measurement

Before gas adsorption measurements, as-synthesized **1**-solvents was soaked in methanol for 3 days to exchange the involved solvents (DMA, ACN and H₂O). Subsequently, the sample was soaked in anhydrous dichloromethane for more than 3 days, during that time fresh dichloromethane was exchanged every day to completely remove methanol solvent. The sample was collected by decanting and dried in air. Before the gas adsorption tests, the dry sample was loaded in a sample tube and further activated under high vacuum at an optimized temperature of 100 °C for 6 h. Finally, 68 mg of degassed sample was used for gas sorption measurements. The gas adsorption isotherm measurements were proceeded at 77 K in a liquid nitrogen bath, at 87 K in a liquid argon bath, at 195 K in a dry ice-acetone bath, at 273 K in an ice-water bath and at 298 K in a water bath.

3. Results and discussion

3.1 Synthesis and crystal structure



Scheme 1 Synthetic procedures and structures of three MOFs with H₃tcpt ligand obtained under different reaction conditions.

We all know that there are a lot of factors which can affect the formation of MOFs, such as reaction solvent, temperature and pH. As shown in Scheme 1, three different MOFs were synthesized by using H_3tcpt ligand under different reaction conditions. $[Zn_3(tcpt)(H_2O)_2] \cdot 3H_2O \cdot TEA \cdot 2DMF$ obtained by Han⁶ is an *AB* packing 2D structure with 41.4% void volume while SNU-100 obtained by Suh⁷ possesses an interpenetrated 3D frameworks with 38.1% solvent accessible volumes. In our work, **1** with a new structural type different from those of above mentioned two MOFs was obtained through a solvothermal reaction of $Zn(NO_3)_2$ and H_3tcpt in a mixed solvent of DMA/ACN/ H_2O with two drops of HBF_4 at 90 °C.

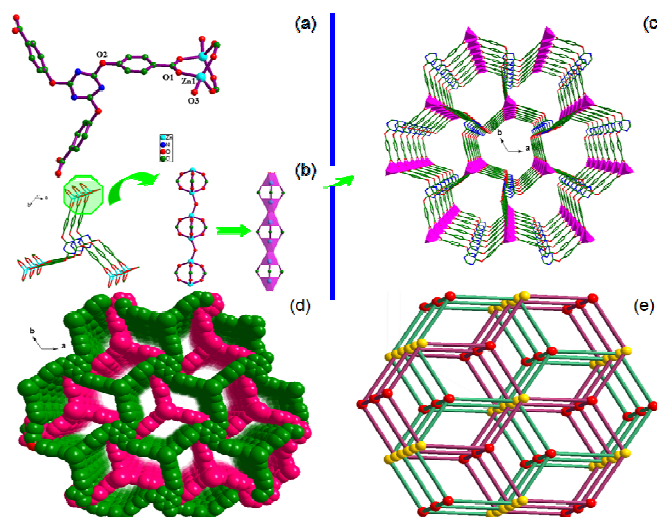


Fig. 1 (a) Coordination environment of the Zn^{2+} in **1**. (All H atoms omitted for clarity). (b) The localized geometry of the $(Zn_2(COO)_3)$ SBU in **1** and polyhedral views of the SBU. (c) View of the hexagonal one-dimensional (1D) channels in a single 3D framework of **1**. (d) Space-filling view of 1D channels in **1** (after interpenetration). (e) Schematic representation of the (3,5) topological net in **1**; the golden balls represent three-connected ligand $tcpt^{3-}$, and the red balls represent the five-connected SBUs.

Single-crystal X-ray structure analysis reveals that **1**-solvents crystallizes in the hexagonal $P6_3/m$ space group and possesses a two-fold interpenetrated 3D framework structure. In the structure of **1**, there exists one crystallographic independent Zn(II) center which is coordinated by three O atoms of carboxylate from three $tcpt^{3-}$ ligands and one O atom of hydroxy (Fig. 1a), and the angle between the triazine ring and benzene ring in $tcpt^{3-}$ ligand is 90°. As shown in Fig. 1b, the two adjacent Zn(II) are bonded together by three carboxylate groups to generate a paddlewheel SBU ($Zn_2(COO)_3$), which is linked by two hydroxy groups to give a five-connected node, as confirmed by solid state 1H NMR (Fig. S7). This node is different from the six-connected SBU node ($Zn_3(COO)_6$) in SNU-100⁷ and $[Zn_3(tcpt)(H_2O)_2] \cdot 3H_2O \cdot TEA \cdot 2DMF$ MOFs.⁶ The Zn–O1 bond length is 1.921(4) Å, which is close to those reported in other zinc-carboxylate compounds.^{5a,6,7,8b,8c} In **1**, each SBU links to three $tcpt^{3-}$ ligands, and each $tcpt^{3-}$ ligand binds three SBUs to form a 2D layer with an irregular hexagonal lattice, which run parallel to the *ab* plane. Interestingly, these 2D layers are linked by O atoms of hydroxy along the *c* axis, which gives rise to a 3D framework (Fig. 1c). Due to the large void, two 3D networks mutually interpenetrate (Fig. 1d), reinforced with each other via intermolecular $\pi \cdots \pi$ (3.4490 Å) interactions between the nearly coplanar central triazine rings. As

a result, the stability of the whole frameworks is further enhanced (as discussed below), and the porosity of this MOF is tuned owing to the hexagonal channels being parted into three smaller rhombic channels with the dimensions of about 4.0×6.4 Å ($a \times b$, taking into account the *van der Waals* radii). By simplifying the organic ligand and the SBU as 3-connected and 5-connected nodes, respectively, the overall structural framework of **1** can be described as a (3,5)-connected infinite 3D *hms* topology (Schlafli symbol $(6^3)(6^9 \cdot 8)$) (Fig. 1e). In addition, the effective free void volume of **1** estimated is about 36.8% (617.4 Å³ out of the 1678.3 Å³ per unit cell volume).

3.2 Stability

Framework stability is one of restrictive factors for the practical application of MOFs. To examine the thermal and water stability of **1**, TGA and PXRD experiments were carried out. The TGA curve of the as-synthesized **1**-solvents reveals a total weight loss of 19.4% before 400 °C, corresponding to the loss of the guest ACN, H_2O and DMA solvent molecules (calculated, 18.7%) following by the decomposition of the compound (a significant weight loss is observed) (Fig. S2b). The TGA curve of solvent (MeOH and CH_2Cl_2) exchanged sample of **1** exhibits the weight loss of 20% from 25 to 140 °C indicating the removal of the new solvent molecules and the framework could remain stable up to 400 °C, followed by the compound decomposition. Compared with the 2D structural $[Zn_3(tcpt)(H_2O)_2] \cdot 3H_2O \cdot TEA \cdot 2DMF$ ⁶ with a thermal stability up to 360 °C, SNU-100⁷ and **1** seemed to be more stable. This might be caused by the SBU stabilization^{28,29}. In the SBU, Zn(II) is four-coordinated in a tetrahedral environment, which is generally a stable configuration for Zn(II) complexes. Moreover, both the discrete SBUs in SNU-100 and **1** were connected to form an infinite chain of linked SBUs, further improving the stability of the SBU and the whole frameworks.

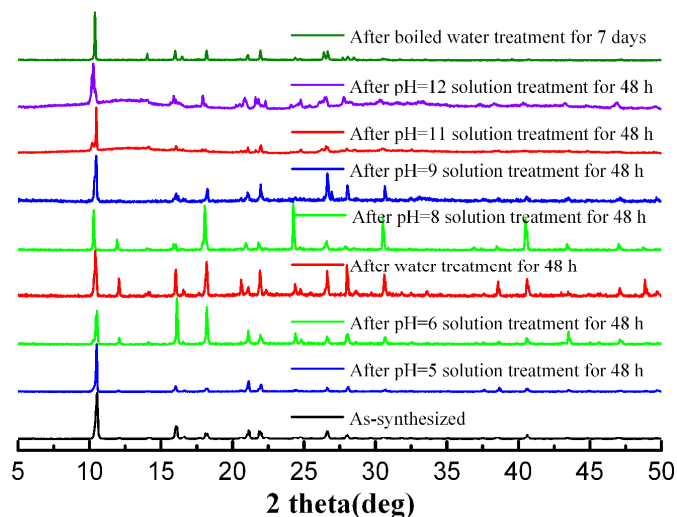


Fig. 2 PXRD patterns of **1** after treated by soaking its samples in pH = 5, 6, 7, 8, 9, 11 and 12 aqueous solutions, respectively for 48 h and boiled water for 7 days.

It should be pointed out that a lot of MOFs can not preserve their framework structures under water environment, because the relative weak coordination bonds could not stand the attack from water molecule, particularly in acid/base conditions, which limits their applications in a lot of fields. Therefore, the stable MOFs are urgent

pursuit.¹⁴ For **1** in this work, firstly it was found that the PXRD patterns of the as-synthesized bulk product, the solvent exchanged sample and the after gas-sorption sample are closely coincident with the simulated pattern derived from the X-ray single crystal data (Fig. S2a), suggesting a good stability against organic solvents and vacuum of this MOF. Then, the PXRD patterns of samples of **1** which were treated by soaking in pH = 5, 6, 7, 8, 9, 11 and 12 aqueous solution, respectively for 48 h were collected (Fig. 2). Interestingly, the resulting patterns still match well with the simulated one, indicating the high water stability, even if in the presence of acid. However, the samples of **1** dissolved aqueous solution with the pH over 13. Another tough condition, soaking the samples of **1** in boiled water, was tested. Surprisingly, this MOF could be stable in boiled water for at least 7 days, as proved by the PXRD (Fig. 2 and Fig. S2e). Furthermore, the CO₂ uptakes of the samples of **1** treated by aqueous solutions with different pH values have no obvious changes when compared with original sample (Fig. 5d), also confirming the excellent framework stability of **1**. The excellent water/acid stability of this MOF may be attributed to the specific SBU and interpenetrated nature in its structure, being beyond a lot of Zn(II)-based MOFs.

3.3 Gas adsorption

Encouraged by the porous structure, the high stability and structural rigidity, N₂ adsorption experiment at 77 K was performed to evaluate the porosity of **1**. The uptake amount of N₂ is 252 cm³ g⁻¹ (STP) at 77 K and 1 atm, and the adsorption shows a reversible type I isotherm (Fig. 3), which is characteristic of the microporous material. The calculated H-K (Horvath-Kawazoe)¹⁵ pore size distributions range from 3.2 to 7.8 Å, being corresponding to the pore sizes evaluated from single-crystal X-ray structure. Based on the N₂ adsorption isotherm, the Brunauer-Emmett-Teller (BET) and Langmuir surface areas of this MOF are estimated to be 905 and 1076 m² g⁻¹, respectively, and the pore volume is 0.306 cm³ g⁻¹, both higher than those for Zn₃(tcpt)(H₂O)₂.

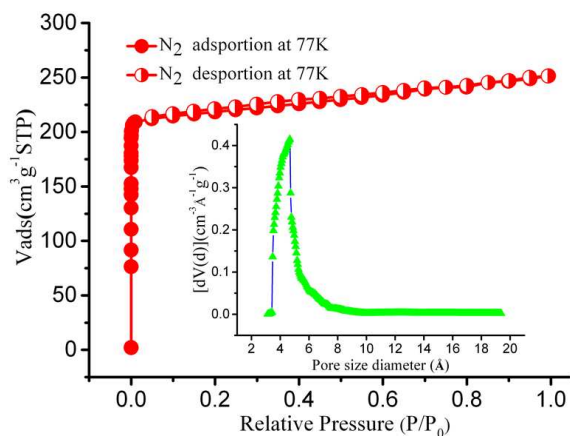


Fig. 3 N₂ sorption isotherms of **1** at 77K (inset, pore size distribution plot).

The permanent porosity and suitable pore size in **1** prompt us to investigate its H₂ storage ability. The adsorption isotherms of H₂ at 77 and 87 K under the pressure up to 1 atm are shown in Fig. 4. It reveals that **1** can adsorb a large amount of H₂ up to 2.21 wt% and 1.52 wt%, respectively at 1 atm. It should be pointed out that the H₂ uptake of **1** is comparable with many reported MOFs like

MOF-177,^{S6} MOF-650,^{S13} SNU-100-M,⁷ and Cu₂(TPPC-OⁿPr)^{S14} in spite of its relative lower void volume (37.7%) and BET surface areas (Table S3). It is noteworthy that the micropore size distributions of **1** is around 5 Å just close to the size about two H₂ molecules (2 × 2.8 Å), which may help enhancing the interaction forces between the H₂ molecules and the framework, thereby benefiting the H₂ adsorption. Moreover, as shown in Fig. S6, interpenetration brought rhombic channels with small open windows (3.66 Å, Fig. S6), which might benefit for the H₂ adsorption.^{7,29,30} Some studies have proved that small pore size is necessary to achieve high H₂ uptake, since the small pore enables the overlap of energy potentials between the opposing walls, leading to higher interaction energy with the H₂ molecules.³¹⁻³⁴ For example, PCN-6 exhibits a higher H₂ uptake than PCN-6', indicating a substantially stronger interaction in the interpenetrated PCN-6, than that in the non-interpenetrated PCN-6'.³⁵ To evaluate the interaction between the adsorbed H₂ molecules and the host framework of **1**, the isosteric heats of adsorption (Q_{st}) of H₂ adsorption were calculated, to be 8.0~6.8 kJ mol⁻¹ depending on the degree of H₂ loading (Fig. S3b), estimated by fitting the H₂ isotherms at 77 and 87 K using a Virial method (Fig. S3a)¹⁶. The initial Q_{st} (8.0 kJ mol⁻¹) is higher than those for some common MOFs such as MOF-5 (4.8 kJ mol⁻¹), because of the small pore size resulting from the structural interpenetration.

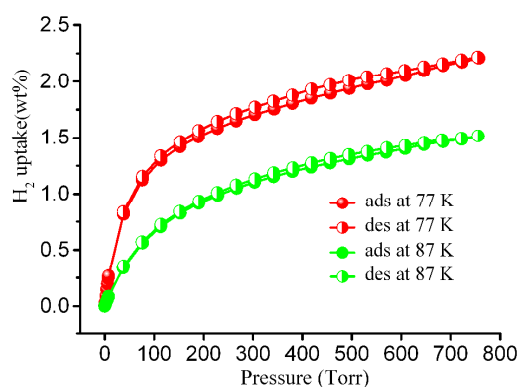


Fig. 4 H₂ sorption isotherms of **1**.

Although non-interpenetrated frameworks usually have large pores and high surface areas suitable for a lot of adsorption-based applications,^{8a,S6,S13} the interpenetrated networks have been proven to be useful in some cases, such as in selective guest captures.^{4b,17-20} Therefore, **1** was further checked for CO₂, CH₄ and N₂ captures. The adsorption isotherm of CO₂ at 195 K is shown in Fig. 5a. Clearly, significant amounts of CO₂ were adsorbed and the isotherm presents typical type I curve, with no obvious change upon repeated cyclings. The adsorption amounts increase abruptly at the low pressure range, up to 150 cm³ g⁻¹ (STP) at 50 torr, and finally up to 205 cm³ g⁻¹ (40.3 wt%) at 1 atm. Approximately 11.6 CO₂ molecules are adsorbed for per cell volume of **1**. Moreover, as shown in Fig. 5b and c, gas adsorptions of **1** exhibit significantly different uptakes towards CO₂, CH₄ and N₂ at both 273 and 298 K. **1** can uptake a moderate amount of CO₂ up to 110.5 cm³ g⁻¹ (273 K) and 71.3 cm³ g⁻¹ (298 K), while the uptake amounts of CH₄ are 45.8 cm³ g⁻¹ (273 K) and 19.9 cm³ g⁻¹ (298 K) at 1 atm. However, at the two temperatures, the uptake amounts of N₂ are only 17.7 and 3.5 cm³ g⁻¹, respectively at 1 atm.

In order to estimate the adsorption selectivities of **1** towards CO₂, CH₄ and N₂, the initial slopes of their adsorption isotherms were calculated at very low pressure ranges (Fig. S5a and b).²¹ The calculated CO₂/CH₄ selectivity is 5.2:1 at 273 K and 5.0:1 at 298 K. Using the same method, the CO₂/N₂ selectivities were calculated to be 19.4:1 at 273 K and 33.6:1 at 298 K, respectively. The selectivity for CO₂ over N₂ at 298 K is indeed comparable to some reported MOFs (Table S4), and higher than BPL carbon which is widely applied in industry for gas separations.³⁶ In addition, to evaluate the interaction between the CO₂ molecules and the host framework, the CO₂ isosteric heats of adsorption (Q_{st}) in **1** was calculated based on the respective adsorption isotherms at 273 K and 298 K. Employing the Clausius-Clapeyron equation,^{22,23} the calculated Q_{st} values range from 31.2 to 40.9 kJ mol⁻¹ depending on the gas loading (Fig. S4). The observed selective sorption behaviors of CO₂ over CH₄ and N₂ may be attributed to the stronger host-guest interaction between the CO₂ molecules with large quadrupole moment and the framework, than other two gases.²⁴⁻²⁷ On the other hand, the framework interpenetration leads to narrow rhombic channels with a size of 4.0 × 6.4 Å. However, the height of rhombic channels is only 3.66 Å (Fig. S6). Given the dynamic radius of these gas molecules, CO₂ (3.3 Å), N₂ (3.64 Å), CH₄ (3.8 Å), dimensional effect may also play an important role for the selective adsorption.

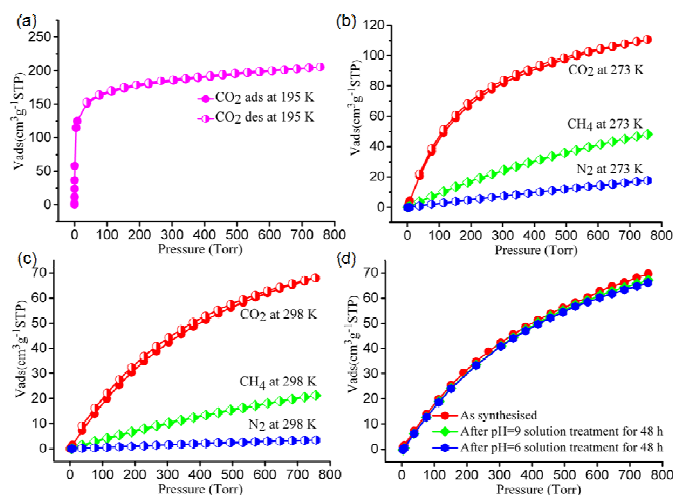


Fig. 5 Gas sorption isotherms for **1**: (a) CO₂ at 195 K. (b) CO₂, CH₄ and N₂ at 273 K. (c) CO₂, CH₄ and N₂ at 298 K. (d) CO₂ at 298 K.

Conclusions

A novel two-fold interpenetrated 3D MOF with rare Zn(II)-based SBU, (Zn₂(COO)₃) has been synthesized under a solvothermal reaction conditions and structurally characterized. Compared with reported Zn(II)-based partners with the same ligand, the synthesis conditions, particularly used solvents played a key role in the formation of different SBUs, thereby distinct MOFs in this system. Particularly, **1** has good thermal and excellent water stability, even if in acid aqueous solution with the pH ranging from 5 to 12. In addition, **1** performs pretty good gas sorption capabilities for H₂ and CO₂, and high adsorption selectivities towards CO₂ over N₂ and CH₄, suggesting its potential applications in gas storage and separation.

Acknowledgement

This work was financially supported by the National Science Foundation of China (21371028).

References

- (a) J. Liu, P. K. Thallapally, B. P. McGrail, D. R. Brown and J. Liu, *Chem. Soc. Rev.*, 2012, **41**, 2308. (b) S.-S. Chen, P. Wang, S. Takamizawa, T.-A. Okamura, M. Chen and W.-Y. Sun, *Dalton Trans.*, 2014, **43**, 6012. (c) J. Yang, X. Wang, R. Wang, L. Zhang, F. Liu, F. Dai and D. Sun, *Cryst. Growth Des.*, 2014, **14**, 6521. (d) K. Na, K. M. Choi, O. M. Yaghi and G. A. Somorjai, *Nano Lett.*, 2014, **14**, 5979. (e) T. Panda, T. Kunduz and R. Banerjee, *Chem. Commun.*, 2012, **48**, 5464. (f) M. Zhu, S.-Q. Su, X.-Z. Song, Z.-M. Hao, S.-Y. Song and H.-J. Zhang, *Dalton Trans.*, 2012, **41**, 13267. (g) Y.-X. Ren, X.-J. Zheng, L.-C. Li, D.-Q. Yuan, M. An and L.-P. Jin, *Inorg. Chem.*, 2014, **53**, 12234. (h) T. Aharen, F. Habib, I. Korobkov, T. J. Burchell, R. Guillet-Nicolas, F. Kleibz and M. Murugesu, *Dalton Trans.*, 2013, **42**, 7795. (i) J.-R. Li, Q. Yu, E. C. Sanudo, Y. Tao and X.-H. Bu, *Chem. Commun.*, 2007, 2602.
- (a) S. J. Yang and C. R. Park, *Adv. Mater.*, 2012, **24**, 4010. (b) D. Bradshaw, A. Garai and J. Huo, *Chem. Soc. Rev.* 2012, **41**, 2344.
- (a) C. Yang, U. Kaipa, Q. Z. Mather, X. Wang, V. Nesterov, A. F. Venero and M. A. Omary, *J. Am. Chem. Soc.*, 2011, **133**, 18094. (b) D.-S. Zhang, Z. Chang, Y.-F. Li, Z.-Y. Jiang, Z.-H. Xuan, Y.-H. Zhang, J.-R. Li, Q. Chen, T.-L. Hu and X.-H. Bu, *Sci. Rep.*, 2013, **3**, 3312.
- (a) Y.-Q. Chen, G.-R. Li, Z. Chang, Y.-K. Qu, Y.-H. Zhang and X.-H. Bu, *Chem. Sci.*, 2013, **4**, 3678. (b) Y. He, Z. Zhang, S. Xiang, F. R. Fronczek, R. Krishna and B. Chen, *Chem. Commun.*, 2012, **48**, 6493.
- (a) X. Zhao, H. He, F. N. Dai, D. Sun and Y. Ke, *Inorg. Chem.*, 2010, **49**, 8650. (b) Z. Wang, B. Zheng, H. Liu, P. Yi, X. Li, X. Yu and R. Yun, *Dalton Trans.*, 2013, **42**, 7850. 11034. (c) A. K. Chaudhari, S. S. Nagarkar, B. Joarder and S. K. Ghosh, *Cryst. Growth Des.*, 2013, **13**, 3716. (d) H. He, F. Sun, T. Borjigin, N. Zhao and G. Zhu, *Dalton Trans.*, 2014, **43**, 3716.
- L. Han, Y. Yan, F. X. Sun, K. Cai, B. Borjigin, X. Zhao, F. Qu and G. Zhu, *Cryst. Growth Des.*, 2013, **13**, 1458.
- H. J. Park and M. P. Suh, *Chem. Sci.*, 2013, **4**, 685.
- (a) S. Zhang, Z. Chang, T.-L. Hu and X.-H. Bu, *Inorg. Chem.*, 2010, **49**, 11581. (b) M.-S. Chen, M. Chen, T. Okamura, W.-Y. Sun and N. Ueyama, *Micropor. Mesopor. Mat.*, 2011, **139**, 25. (c) Z.-Q. Shi, Z.-J. Guo and H.-G. Zheng, *Chem. Commun.*, 2015, **51**, 8300.
- C. B. Aakeroy, J. Desper and J. F. Urbina, *CrystEngComm*, 2005, **7**, 193.
- CrysAlis RED, Oxford Diffraction Ltd., Version 1.171.29.2.
- G. M. Sheldrick, *Acta Cryst.* 2015, **C71**, 3-8.
- L. J. Farrugia, *J. Appl. Cryst.* 1999, **32**, 837.
- O. V. Dolomanov, L. J. Bourhis, R. J. Gildea, J.A.K. Howard and H. J. Puschmann, *Appl. Cryst.* 2009, **42**, 339-341.
- (a) J. Yang, A. Grzech, F. M. Mulderb and T. J. Dingemans, *Chem. Commun.*, 2011, **47**, 5244. (b) J. J. Low, A. I. Benin, P. Jakubczak, J. F. Abrahamian, S. A. Faheem and R. R. Willis, *J. Am. Chem. Soc.*, 2009, **131**, 15834. (c) H. J. J. Walton, *Dalton Trans.*, 2013, **42**, 15421. (d) J. H. Im, N. Ko, S. J. Yang, H. J. Park, J. Kim and C. R. Park, *New J. Chem.*, 2014, **38**, 2752.
- G. Horvath and K. Kawazoe, *Chem. Eng. Jpn.*, 1983, **16**, 470.
- L. Czepirski and J. Jagiello, *Chem. Eng. Sci.*, 1989, **44**, 797.

17. Y.-W. Li, L.-F. Wang, K.-H. He, Q. Chen and X.-H. Bu, *Dalton Trans.*, 2011, **40**, 10319.
18. S.-Q. Ma, X.-S. Wang, E. S. Manis, C. D. Collier and H.-C. Zhou, *Inorg. Chem.* **2007**, *46*, 3432.
19. H. Kim and M. P. Suh, *Inorg. Chem.*, 2005, **44**, 810.
20. S. Bureekaew, H. Sato, R. Matsuda, Y. Kubota, J. Kim, K. Kato, M. Takata and S. Kitagawa, *Angew. Chem., Int. Ed.*, 2010, **49**, 7660.
21. J. An, S. J. Geib and N. L. Rosi, *J. Am. Chem. Soc.*, 2010, **132**, 38.
22. D. Zhong, J. Lin, W. Lu, L. Jiang and T. Lu, *Inorg. Chem.*, 2009, **48**, 8656.
23. M. Dincă and J. R. Long, *J. Am. Chem. Soc.*, 2005, **127**, 9376.
24. J.-R. Li, J. Sculley and H.-C. Zhou, *Chem. Rev.*, 2012, **112**, 869.
25. Y. Qin, X. Feng, F. Luo, G. Sun, Y. Song, X. Tian, H. Huang, Y. Zhu, Z. Yuan, M. Luo, S. Liu and W. Xu, *Dalton Trans.*, 2013, **42**, 50.
26. J.-B. Lin, J.-P. Zhang and X.-M. Chen, *J. Am. Chem. Soc.*, 2010, **132**, 6654.
27. J. Lincke, D. Lässig, M. Kobalz, J. Bergmann, M. Handke, J. Möllmer, M. Lange, C. Roth, A. Möller, R. Staudt and H. Krautscheid, *Inorg. Chem.*, 2012, **51**, 7579.
28. D. Sun, Y. Ke, D. J. Collins, G. A. Lorigan and H.-C. Zhou, *Inorg. Chem.*, 2007, **46**, 2725.
29. D. Zhao, D. J. Timmons, D. Yuan and H.-C. Zhou, *Acc. Chem. Res.*, 2010, **44**, 123.
30. L. Pan, M. B. Sander, X. Huang, J. Li, M. Smith, E. Bittner, B. Bockrath and J. K. Johnson, *J. Am. Chem. Soc.*, 2004, **126**, 1308.
31. M. P. Suh, H. J. Park, T. K. Prasad and D.-W. Lim, *Chem. Rev.*, 2012, **112**, 782.
32. D. H. Everett and J. C. Powl, *J. Chem. Soc., Faraday Trans.*, 1976, **72**, 619.
33. D. Zhao, D. Yan and H.-C. Zhou, *Energy Environ. Sci.*, 2008, **1**, 225.
34. B. Kesanli, Y. Cui, M. R. Smith, E. W. Bittner, B. C., Bockrath and W. Lin, *Angew. Chem., Int. Ed.*, 2005, **44**, 72.
35. (a) S.-Q. Ma, D. Sun, M. Ambrogio, J. A. Fillinger, S. Parkin and H.-C. Zhou, *J. Am. Chem. Soc.*, 2007, **129**, 1858; (b) S.-Q. Ma, J. Eckert, P. M. Forster, J. W. Yoon, Y. K. Hwang, J.-S. Chang, C. D. Collier, J. B. Parise and H.-C. Zhou, *J. Am. Chem. Soc.*, 2008, **130**, 15896.
36. M. G. Nijkamp, J. E. M. J. Raaymakers, A. P. van Dillen and K. P. de Jong, *Appl. Phys. A: Mater. Sci. Process.*, 2001, **72**, 619.

Graphical Abstract

A Hydrothermal Stable Zn(II)-based Metal-Organic Framework: Structural Modulation and Gas Adsorption

Xiuling Zhang, Yong-Zheng Zhang, Da-Shuai Zhang, Baoyong Zhu, Jian-Rong Li

A hydrothermal stable MOF, $[\text{Zn}_2(\text{tcpt})\text{OH}] \cdot \text{solvents}$ (**1**·solvents) was synthesized, in which an unusual paddlewheel SBUs $\text{Zn}_2(\text{COO})_3$ was found. Furthermore, **1** can adsorb considerable amounts of H_2 and displays high selective adsorption of CO_2 over N_2 .

